

Bond of self-compacting concrete incorporating silica fume: Top-bar effect, effects of rebar distance from casting point and of rebar-to-concrete relative displacements during setting



Konstantinos G. Trezos, Ioannis P. Sfikas*, Konstantinos Orfanopoulos

National Technical University of Athens, Greece, School of Civil Engineering, Laboratory of Reinforced Concrete 5, Iroon Polytechniou, 157 73 Zografou Campus, Greece

HIGHLIGHTS

- The top-bar effect is eliminated for SCC incorporating 8.9–10.6% silica fume.
- No bond loss was observed in SCC up to 1.60 m from the single casting point.
- The bond variation is comparable between SCC and NVC.
- Setting depends on superplasticizer content, regardless of the concrete type.
- Rebar displacements during setting similarly affect SCC and NVC bond.

ARTICLE INFO

Article history:

Received 24 January 2014

Received in revised form 10 June 2014

Accepted 27 September 2014

Available online 19 October 2014

Keywords:

Silica fume

Bond

Setting

Displacements

ABSTRACT

This study investigates the effect of different silica fume levels of cement replacement on the bond capacity of Self-Compacting Concrete (SCC).

Specifically, the top-bar effect, the bond variation as a function of the rebar distance from the casting point and the effect of a rebar-to-concrete relative displacement during setting on bond are examined. Vertical and horizontal specimens with transverse rebars distributed over height (600 mm) and length (1780 mm), respectively, were cast and tested by pull-out. Six SCC mixtures with various replacement levels were investigated and compared to one reference SCC mixture (without silica fume) and three Normally Vibrated Concrete (NVC) mixtures of different workability classes.

It was found that the top-bar effect of SCC mixtures incorporating silica fume is less intense than in NVC and it is almost eliminated for replacement levels between 8.9% and 10.6% (by weight). No bond loss is evident up to at least 1.60 m from the casting point. Finally, the effect of a rebar-to-concrete relative displacement during setting on bond is similar between SCC and NVC. Although higher initial setting times are observed in SCC, bond is not prone to reduction due to a rebar-to-concrete relative displacement during this period.

© 2014 Elsevier Ltd. All rights reserved.

1. Introduction

The increased reinforcement requirements that have been adopted by major building codes [1–2] during the last three decades have led to considerably high congested concrete members. As a result of the required dense reinforcement, significant difficulties have been encountered, regarding the correct application and the effectiveness of the mechanical compaction, in order to adequately fill the formworks, without leaving any surface or hidden

voids. Thus, the uniformity of the final material during the execution of Normally Vibrated Concrete (NVC) structures has been put into question, up to some extent.

In the late 1980's, Self-Compacting Concrete (SCC) had been universally introduced [3–6] as a revolutionary material that had the ability to easily flow under its own weight and adequately fill highly congested concrete members, without requiring any compaction. Since then, the enhanced rheological properties of SCC have been admired in practice by the construction industry and its use has been widely extended. Concurrently, a great number of researchers on a worldwide scale have been motivated to further investigate the effects of using SCC on several hardened concrete properties, such as mechanical strength and durability.

* Corresponding author. Tel.: +30 210 772 1210 (O); fax: +30 210 772 4008.

E-mail addresses: ctrezos@central.ntua.gr (K.G. Trezos), gsfikas@gmail.com (I.P. Sfikas), korfanop@gmail.com (K. Orfanopoulos).

Bond to reinforcement steel is considered to be one of the most crucial mechanical properties, as it is directly associated with the ability of reinforced concrete to act as a composite material by ensuring the cooperation between steel and the surrounding concrete. Previous research has already provided sufficient data to give confidence in the bond behaviour of SCC. Specifically, it has found that the normalized bond strength of SCC is, in general, similar or higher than of NVC [7–14] and it usually presents a lower scatter [11,13–16]. However, limited attention has yet been given to the effect of the specific composition properties on the resulting bond, whilst a further investigation on more specialized bond issues is also potentially critical.

The incentive of the present study is to supplement previous literature on the effect of SCC composition on advanced aspects of bond. Specifically, the impact of (i) the rebar position over height (top-bar effect), (ii) the rebar distance from the casting point and (iii) a rebar-to-concrete relative displacement during setting, as a result of possible unintentional formwork displacements, on bond was examined in six SCC mixtures, produced with various silica fume levels of cement replacement. The results were compared to the corresponding bond characteristics of one reference SCC mixture (without silica fume) and three typical NVC mixtures.

2. Theoretical approach

2.1. Effect of composition

As it has been formerly reported [8,12,14,17–19], the quality of concrete, in terms of its composition, its production process and its placing method, may significantly affect bond capacity. It is considered [7,14,19–23] that any changes in composition that affect the morphology of the concrete matrix may lead to considerable effects in bond characteristics. Such composition changes include variations in the content of cement, water or any supplementary inert, pozzolanic or hydraulic materials (type I or II additions), the latter being frequently used for the production of rheologically enhanced and stable SCC mixtures.

For silica fume in NVC, the bond-enhancing effect has been previously discussed in several studies [18,20,24–27]. The enhanced bond has been attributed to both the chemical reaction between CH crystals and the pozzolanic material (pozzolanic reaction) and the filling effect (physical action) that are considered to significantly densify the concrete-steel transition zone and, thus, reduce the accumulation of free water due to bleeding under the horizontally placed rebars. Combined with the usually lower water content of SCC mixtures, the achieved denser capillary network is expected to reduce the water accumulation beneath all rebars, thus enhance bond behaviour.

2.2. Effect of rebar position over height (top-bar effect)

For deep concrete members and apart from the concrete composition, the role of reinforcement, and, specifically, the effect of the rebar orientation and position on the resulting bond capacity, is considered to be significant. For NVC, major building codes [1–2] have adopted a correction factor that decreases the value of bond strength in the higher parts of the deep concrete members.

This correction factor aims to confront the phenomenon, known as the 'top-bar effect', whose mechanism can be summarized as follows. Prior to the final setting (stiffening) of concrete, the heavier constituent materials (cement, aggregates) tend to settle due to gravity (plastic settlement), thus forcing the lighter water to move upwards, through the capillary network, to the higher parts

of the concrete members and, finally, their free surface (bleeding phenomenon). Along this path, part of the water is trapped underneath the horizontal reinforcement bars, thus reducing the quality of the interface zone, in terms of the bonding between steel bars and the surrounding concrete. This water accumulation is higher in the upper parts of deep concrete members. In addition to this mechanism, the air entrapment underneath the reinforcement bars and between their ribs due to the vibration process of NVC is also known to further negatively influence the resulting bond.

As explained previously (Section 2.1), the more densified capillary network of SCC, due to the incorporation of both inert and/or pozzolanic additions, leads to a reduction of the water accumulation beneath bars, and, therefore, the top-bar effect is expected to be less significant.

This significance has been previously investigated by several researchers [10–12,15–17,21,22,27–30] and it has been reported that SCC behaviour is either equal or better than NVC for high elements and the top-bar effect is less intense for SCC mixtures. Furthermore, many researchers implied that the provisions of EN 1992-1-1 (2004) [1] for NVC appear to be adequate for SCC [9,11,14,21,27]. However, it has been also reported [9,15] that the bond reduction with height exceeded these provisions in some SCC and NVC specimens, up to some extent. It should be noted that each of these studies focuses on different parameters (concrete strength, rheology characteristics, cover thickness, bond length, etc.) and they should not be directly compared.

2.3. Effect of distance from the casting point

Another major issue that has yet been limitedly investigated is the effect of the rebar distance from the casting point on bond characteristics. The ability of SCC to flow over considerably greater distances (compared to NVC) with insignificant or no signs of obvious segregation, offers the advantage of reducing the required casting points during the execution of a structure. In ACI 237R (2007) [31], the concrete discharge at one single casting point is suggested until either the concrete member is completely filled (beams) or the fresh mixture has flown as far as possible, before moving the point of discharge (slabs).

Given the satisfactory segregation resistance of properly designed SCC mixtures, an insignificant bond loss across length should be expected, yet there is only limited research work to validate this assumption. Previous work [13,29] has shown that some issues may arise especially for lower slump-flow values and for greater distances from the casting point. Still, it is considered that the dominant cause of the reduced bond is not a local deterioration in the concrete-steel interface zone but the unsuccessful embedment of rebars, in terms of the reduced steel cover in remote regions due to the decreasing slope of the final surface. In both studies, the low concrete cover in higher distances led a great number of rebars to fail by splitting, instead by pull-out.

2.4. Effect of rebar displacements during concrete setting

During concrete setting, a possible local differential settlement of formwork's scaffolding or a horizontal formwork displacement due to a seismic event or a blast load may result in a relative displacement between the embedded rebars and the surrounding concrete. The effect of such a rebar-to-concrete relative displacement on the particle interlocking of aggregates within the concrete matrix may be reflected on bond; however no previous research work has been conducted on the subject.

3. Concrete mixtures & materials

3.1. Concrete mixtures

In total, ten concrete mixtures were cast and tested: seven SCC and three NVC mixtures. The mixture proportions for all mixtures are shown in Table 1. The total nominal weight, the unit weight coefficient (ratio of total actual weight per cubic meter, as calculated in a mould of known volume, to total nominal weight) and the cube compressive strength are also reported in this Table.

All SCC mixtures were based on a common composition, characterized by same binder (total content of cement and silica fume), limestone powder, total aggregate and water content. The polycarboxylic ether (*pce*) content was suitably adjusted in order for all mixtures to reach similar fresh concrete properties (flowability, viscosity and stability). The only variation adopted were the relevant proportions between silica fume and cement (for the same total binder content), in order to underline the effect of silica fume level of cement replacement on the examined bond properties.

The NVC mixtures were designed on the basis of a typical composition used in the local construction industry and they represent different slump categories (S1, S2 and S4, with respect to EN 206 (2013) [32]), which were achieved by incorporating different levels of superplasticizer. The water content is higher than for SCC mixtures, as it was selected according to the common practice of the local commercial NVC mixtures.

3.2. Constituent materials

Cement (*c*) – For the production of all concrete mixtures, a typical Portland composite cement was used (CEM II / B-M (P-W-L) 42.5 N), with a nominal strength category of 42.5 N/mm² and with sulphate resistance properties and moderately low heat of hydration, conforming to EN 197-1 (2011) [33]. The cement grading curve is presented in Fig. 1, comparatively to the corresponding curves of the other fine materials used for the purposes of the current study (silica fume, limestone powder). The cement content was set to 350 kg/m³ for the reference mixture SCC1 and was gradually decreased for mixtures with higher silica fume replacement levels, in order to attain a constant binder content (cement and silica fume) of 350 kg/m³. For NVC mixtures, the cement content was uniformly set to 400 kg/m³.

Silica fume (*sf*) – The incorporated silica fume is a very active pozzolan in the form of fine powder (Fig. 1) and it was used as a replacement of the initial quantity of cement (350 kg/m³ for reference mixture SCC1, which is equal to the total binder, *b*, of each SCC mixture) at six levels, i.e. *sf/b* = 4.9%, 6.9%, 8.9%, 10.6%, 12.3% and 14.0% (by weight). The physical properties and the chemical analysis (percentage weight by total weight, % w/w) of *sf* are shown in Table 2. It should be noted that, although the density of silica fume (2.20 t/m³) is considerably lower than the corresponding density of the replaced cement (assumed in the range of 3.10–3.15 t/m³, though not calculated or provided by the producer) the final concrete volume was not significantly influenced, due to the limited amount of replacement compared to the total volume of concrete. This can be also observed by the estimated unit weight coefficients (as defined in Section 3.1), which are all close to 1.00 (Table 1). Any deviations of the unit weight coefficients (mainly up to +3%) are not considered significant and are attributed to the experimental procedure and to scaling effects.

Aggregates – Three gradings of locally available crushed calcareous limestone aggregates were used for the production of all mixtures: sand (*s*) 0/4 mm, small gravel (*g1*) 4/8 mm and medium gravel (*g2*) 8/16 mm. The physical properties of the used aggregates are listed in Table 3 and the corresponding grading curves

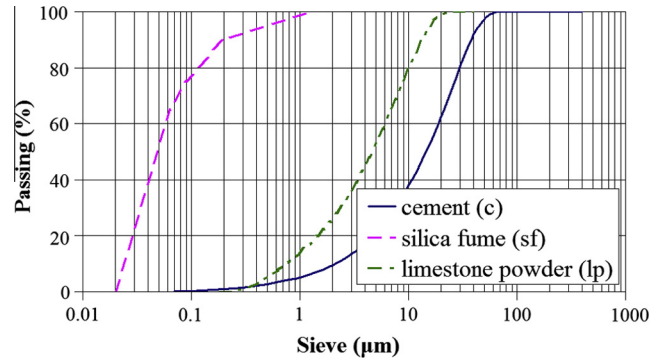


Fig. 1. Grading curves of fine materials: cement, silica fume, limestone powder.

are shown in Fig. 2. The SCC and NVC aggregate mixture grading curves are also shown in the same figure. All suitable corrections were adopted for the aggregates to reach the saturated-surface-dry (SSD) state, according to EN 1097-6 (2000) [34].

Limestone powder (*lp*) – The enhancement of the plastic viscosity characteristics and the required stability of SCC mixtures were achieved by the incorporation of limestone powder of 97.6% calcium carbonate (CaCO₃) purity and high fineness (Fig. 1). The physical properties and the mineralogical composition (percentage weight by total weight, % w/w) of limestone powder are shown in Table 4. The limestone powder content was uniformly set to 175 kg/m³ for all SCC mixtures.

Superplasticizer (*pce*) – Suitable dosages of polycarboxylic ether superplasticizer, conforming to Tables 11.1 and 11.2 of EN 934-2 (2009) [35], were introduced to all mixtures, in order to reach the desired fluidity.

3.3. Reinforcement steel

Deformed steel bars of grade B500C, conforming to EN 10080 (2005) [36], were embedded in the concrete specimens in order to evaluate the bond characteristics. It should be noted that, as reported in recent literature [12,19,22,37,38], the effect of bar diameter on bond can be considerable. Specifically, it has been found that lower diameters lead to higher bond strengths for SCC (compared to NVC), a phenomenon that tends to eliminate for higher diameters. However, for the experimental purposes of the present study, only one bar diameter was tested.

Specifically, all steel bars originated from the same batch and had a nominal diameter, *d_{nom}*, of 16 mm, which represents “medium diameters” (nominal diameters ranging from 10 to 20 mm), according to Table D.1 of EN 10080 (2005) [36].

A typical steel bar, as shown in Fig. 3, has two rows of transverse ribs, which are uniformly distributed on the circumference and are equally spaced along the length of the bar. The transverse ribs resemble the shape of a crescent and they smoothly merge into the core of the steel bar. The projection of the transverse ribs extends at least 75% over the bar perimeter (πd_{nom}).

Five random bar segments have been examined and tested in the laboratory, in order to confirm the producer's technical specifications, regarding the corresponding diameter, section and mass (Table 5), as well as the mechanical characteristics (Table 6). The geometry of the surface and of the transverse ribs (Table 7) has been tested on three bar segments (resulting values are the average of twelve measurements, i.e. four measurements on each rebar).

Table 1
Mixture proportions per cubic meter (kg/m³), unit weight coefficient and cube compressive strengths, *f_{cc}* (N/mm²).

| Description | SCC1 | SCC2 | SCC3 | SCC4 | SCC5 | SCC6 | SCC7 | NVC1 | NVC2 | NVC3 |
|---|------|------|------|------|------|------|------|------|------|------|
| Cement, <i>c</i> | 350 | 333 | 326 | 319 | 313 | 307 | 301 | 400 | 400 | 400 |
| Effective water, <i>w</i> | 178 | 178 | 178 | 178 | 178 | 178 | 178 | 204 | 204 | 204 |
| Limestone powder, <i>lp</i> | 175 | 175 | 175 | 175 | 175 | 175 | 175 | – | – | – |
| Silica fume, <i>sf</i> | – | 17 | 24 | 31 | 37 | 43 | 49 | – | – | – |
| Medium gravel 8/16, <i>g2</i> | 350 | 350 | 350 | 350 | 350 | 350 | 350 | 375 | 375 | 375 |
| Small gravel 4/8, <i>g1</i> | 150 | 150 | 150 | 150 | 150 | 150 | 150 | 200 | 200 | 200 |
| Sand 0/4, <i>s</i> | 1050 | 1050 | 1050 | 1050 | 1050 | 1050 | 1050 | 1050 | 1050 | 1050 |
| PCE superplasticizer, <i>pce</i> | 6.9 | 7.3 | 5.1 | 5.2 | 6.8 | 6.1 | 8.8 | 0.0 | 0.5 | 2.0 |
| Water/binder ratio, <i>w/b</i> | 0.51 | 0.51 | 0.51 | 0.51 | 0.51 | 0.51 | 0.51 | 0.51 | 0.51 | 0.51 |
| Silica fume level, <i>sf/b</i> (%) | – | 4.9 | 6.9 | 8.9 | 10.6 | 12.3 | 14.0 | – | – | – |
| Total nominal weight, <i>W_{nom}</i> | 2243 | 2240 | 2238 | 2238 | 2239 | 2239 | 2241 | 2229 | 2230 | 2231 |
| Total actual weight, <i>W_{act}</i> | 2230 | 2265 | 2236 | 2173 | 2143 | 2182 | 2169 | 2168 | 2194 | 2127 |
| Unit weight coefficient, <i>W_{nom}/W_{act}</i> | 1.01 | 0.99 | 1.00 | 1.03 | 1.04 | 1.03 | 1.03 | 1.03 | 1.02 | 1.05 |
| Cube compressive strength, <i>f_{cc}</i> | 58.7 | 52.9 | 54.3 | 58.4 | 63.3 | 65.2 | 65.5 | 49.7 | 50.7 | 48.6 |
| Standard deviation, <i>sd</i> | 0.2 | 2.0 | 1.8 | 0.1 | 2.2 | 0.2 | 3.0 | 0.8 | 1.0 | 1.9 |

Table 2
Physical properties and chemical analysis (% w/w) of silica fume.

| Physical properties | | Chemical analysis | | | | | | | | |
|-----------------------------|---|-------------------|--------------------------------|------|-----------------|------|--------------------------------|------------------|-------------------|------|
| Density (t/m ³) | Specific surface area – BET (m ² /g) | SiO ₂ | Al ₂ O ₃ | CaO | SO ₃ | Cl | Fe ₂ O ₃ | K ₂ O | Na ₂ O | LOI. |
| 2.20 | 24.2 | 96.40 | 0.75 | 0.35 | 0.05 | 0.01 | 0.56 | 0.43 | 0.04 | 3.01 |

Table 3
Physical properties of aggregates.

| Type | Symbol | Apparent density on an oven dried basis (t/m ³) | Water absorption (%) |
|---------------|--------|---|----------------------|
| Sand | s | 2.66 | 0.9 |
| Small gravel | g1 | 2.66 | 1.1 |
| Medium gravel | g2 | 2.65 | 1.0 |

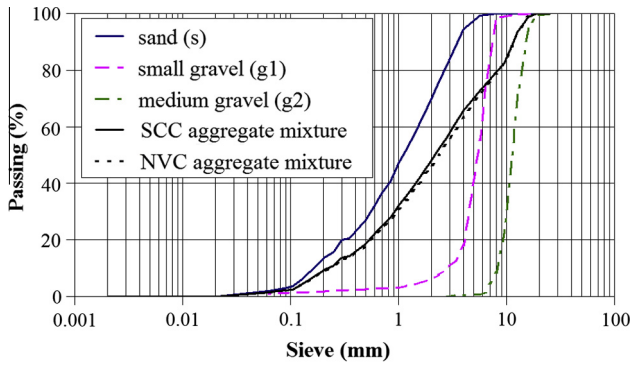


Fig. 2. Grading curves of aggregates and aggregate mixtures.

Table 4
Physical properties and mineralogical composition (% w/w) of limestone powder.

| Physical properties | | | Mineralogical composition (% w/w) | | | |
|-----------------------------|--|--------------|-----------------------------------|------------------|------|--------------------------------|
| Density (t/m ³) | Specific surface area ^a (m ² /g) | Moisture (%) | CaCO ₃ | SiO ₂ | MgO | Fe ₂ O ₃ |
| 2.70 | 1.27 | 0.21 | 97.60 | 0.83 | 0.76 | 0.09 |

^a Calculated from the grain size analysis.

Table 5
Diameter, section and mass of steel bars.

| Parameter | Symbol | Units | Nominal values | | Measured values | |
|-----------|----------------------|-----------------|----------------|------------------|-----------------|---------------|
| | | | Average | Tolerance | Average | St. deviation |
| Diameter | <i>d</i> | mm | 16 | n/a ^a | 15.93 | 0.06 |
| Section | <i>A_n</i> | mm ² | 201 | 4.5% | 199.33 | 1.53 |
| Mass | | kg/m | 1.58 | n/a ^a | 1.56 | 0.01 |

^a n/a: not available.

4. Experimental procedures

4.1. Fresh concrete production, testing & classification

A fixed-pan planetary type cylindrical mixer with rotating blades was used for the production of all mixtures and the same mixing procedure was carefully followed. At first, the aggregates were dry-mixed and then the limestone powder

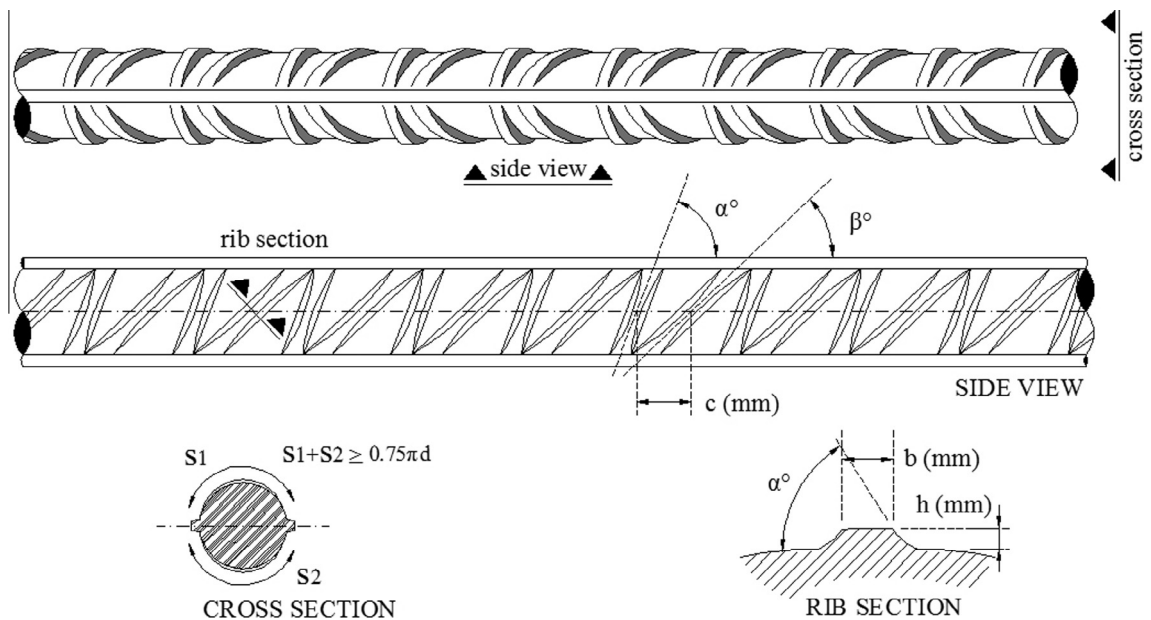


Fig. 3. Typical steel bar sketch and notations.

Table 6
Mechanical characteristics of steel bars (grade B500C).

| Parameter | Symbol | Units | Producer Limits | Measured values | |
|--------------------|-----------------------|-------------------|------------------|-----------------|---------------|
| | | | | Average | St. deviation |
| Yield strength | f_y | N/mm ² | ≥ 500 | 553.00 | 3.81 |
| Tensile strength | f_t | N/mm ² | ≥ 550 | 650.60 | 16.27 |
| Ratio | f_t/f_y | – | ≥ 1.15 ≤ 1.35 | 1.18 | 0.02 |
| Uniform elongation | $\epsilon_{u,k}$ | % | ≥ 8.0 | 10.58 | 0.79 |
| Ratio | $f_{y,act}/f_{y,nom}$ | – | ≤ 1.25 | 1.11 | 0.01 |

Table 7
Surface and transverse ribs geometry of steel bars ($d_{nom} = 16$ mm).

| Parameter | Symbol | Unit | Producer Limits | Measured values | |
|-------------------|----------|---------|---------------------|-----------------|---------------|
| | | | | Average | St. deviation |
| Flank inclination | α | degrees | ≥ 45° | 53.9° | 1.0° |
| Pitch angles | β | degrees | ≥ 35° | 38.4° | 1.2° |
| Height | h | mm | ≤ 75° | | |
| Spacing | c | mm | ≥ 0.03 $d = 0.48$ | 1.10 | 0.2 |
| | | | ≤ 0.15 $d^a = 2.40$ | | |
| Width | b | mm | ≥ 0.4 $d = 6.40$ | 11.00 | 0.5 |
| | | | ≤ 1.2 $d = 19.20$ | | |
| | | | 0.1 $d = 1.60$ | 1.6 | ~0.0 |

^a Also valid for longitudinal ribs.

was added and all ingredients were further dry-mixed. Subsequently, the cement was introduced to the homogeneous dry mixture. Then, 80% of the total water content was added, followed by the rest 20% of the water, in addition with the superplasticizer. The batches were cast at an average temperature of 22 °C and an average relative humidity of 50%.

The evaluation of the fresh concrete behaviour of SCC was performed by four different tests on fresh concrete. Specifically, the workability (unconfined flowability) of all SCC mixtures was assessed by the Slump-flow test that was conducted in accordance with EN 12350-8 (2010) [39]. The evaluation method of the Fresh Visual Stability Index, *FVSI*, as described by ASTM C1611 (2007) [40], was applied for the assessment of the segregation tendency of the mixtures. The viscosity was evaluated by the V-Funnel test, which was conducted according to EN 12350-9 (2010) [41]. Finally, the passing ability was assessed by the L-Box test, which was performed as described by EN 12350-10 (2010) [42]. Then, the mixtures were classified in accordance with the provisions of the European Guidelines for SCC. The concrete workability for NVC was assessed by the standard Slump test, as described by EN 12350-2 (2009) [43], and the mixtures were classified according to EN 206 (2013) [32]. The unit weight coefficient of all mixtures (Table 1) was assessed by following the procedures that are described in ASTM C138 (2001) [44].

The SCC mixtures were designed and cast, aiming at a low/medium slump-flow (SF1/SF2), a high viscosity class (VS1 or VF1) and a high passing ability class (PA2). In addition, all mixtures were designed to be stable and show minor or no dynamic segregation tendency (as defined by *FVSI*). As reported earlier (Section 3.1), the *pce* content was suitably adjusted to achieve the targeted fresh behaviour. Therefore, the effect of *sf* on the fresh properties will not be directly distinguishable and, thus, not further discussed. The NVC mixtures design aimed at three different workability classes.

4.2. Casting and description of specimens

The concrete specimens were cast in accordance with the specifications set by the European Guidelines for SCC [45] for SCC mixtures and by EN 12390-2 (2009) [46] and EN 13670 (2009) [47] for NVC mixtures. Specifically, SCC specimens were cast in one continuous lift without mechanical compaction, whilst NVC specimens were filled in two or three layers, each being followed by adequate mechanical vibration, either on an electric motor vibrating table (for the compressive strength cubic specimens) or by using a concrete mechanical vibrator (for all bond specimens).

For the determination of the compressive strength, three standard cubes (150 × 150 × 150 mm) were cast for each concrete mixture, using standard steel moulds. In total, 30 standard cubes were cast for all mixtures.

For the assessment of the bond capacity, 600 mm high vertical specimens and 1780 mm long horizontal specimens, each with a cross-section of 200 × 200 mm, were used. The bond specimens were produced in plywood moulds. It is recognised that by producing a single specimen for each test type per mixture does not allow the evaluation of the potential dispersion of the assumed mean value of the investigated parameters within the same mixture. However, any possible significant

errors of the mean values are considered to be traceable by evaluating the whole series of mixtures as a group. Further targeted research is required to estimate the dispersion within the same mixture.

As shown in Fig. 4, horizontal transverse deformed steel bars (grade B500C, $d_{nom} = 16$ mm, Section 3.3) were embedded to various predefined positions of the vertical and horizontal moulds, so that the concrete casting direction is perpendicular to the steel rebar. In each rebar position, the steel rebar extended beyond the two opposite sides of the mould. The required effective bond length of 80 mm ($5 \times d_{nom}$) was achieved by attaching 120 mm long plastic sleeves around the remaining part of the rebar length inside the cross-section. The tolerance of the sleeves around the steel bars reached about 1 mm, whilst their thickness did not exceed 1 mm. The plastic sleeves were adjusted into place and sealed with sealant material (plasticine), in order to avoid the inflow of cement paste into the encased reinforcement.

In total, ten vertical specimens (with three rebars distributed every 200 mm over height, starting from 100 mm from the bottom, and symbolized as B_{bot} , B_{mid} and B_{top} for the bottom, the middle and the top rebar, respectively) and seven horizontal specimens (with nine rebars evenly distributed every 200 mm across length, starting from 80 mm from the casting point edge, and symbolized as $B1$ to $B9$, starting from the same edge) were cast for the purposes of the current study (Table 8).

All specimens were left to set for 20 h after casting and, after being demoulded, they were air cured at uncontrolled but practically constant ambient conditions (temperature of approximately 20 ± 2 °C and relative humidity of approximately 50%), until the age of testing (28 days).

4.3. Concrete setting

The concrete setting was estimated on the basis of ASTM C 403 (1999) [48], with the difference that the penetration resistance, *PR* (N/mm²), was measured on the concrete specimens, instead of on a separate mortar sample, obtained by sieving. This variation can be considered as acceptable, as the maximum aggregate size used (16 mm) was significantly smaller than in ordinary concrete (32 mm), for which the standard was designated, and any local irregularities were spotted and eliminated by taking more measurements than the single one predicted. Specifically, five measurements were taken, which were equally distributed across the length of the horizontal specimen, and their average value was calculated. Any measurements deviating more than 10% from the average value were discarded and a new average value was calculated.

The followed procedure consisted of the recording of concrete resistance to penetration by standard smooth needles of three diameters (6, 8 and 16 mm). The needle is uniformly penetrated to concrete to a predefined depth (marked on needle surface) at constant rate and duration. The force required for the penetration and the time of application, measured as the elapsed time after initial mixing of cement and water, are recorded. From a plot of *PR* versus the elapsed time, the times of initial, t_m (min), and final setting, t_{fm} (min), can be determined as the times corresponding to *PR* equal to 3.5 and 27.6 N/mm², respectively.

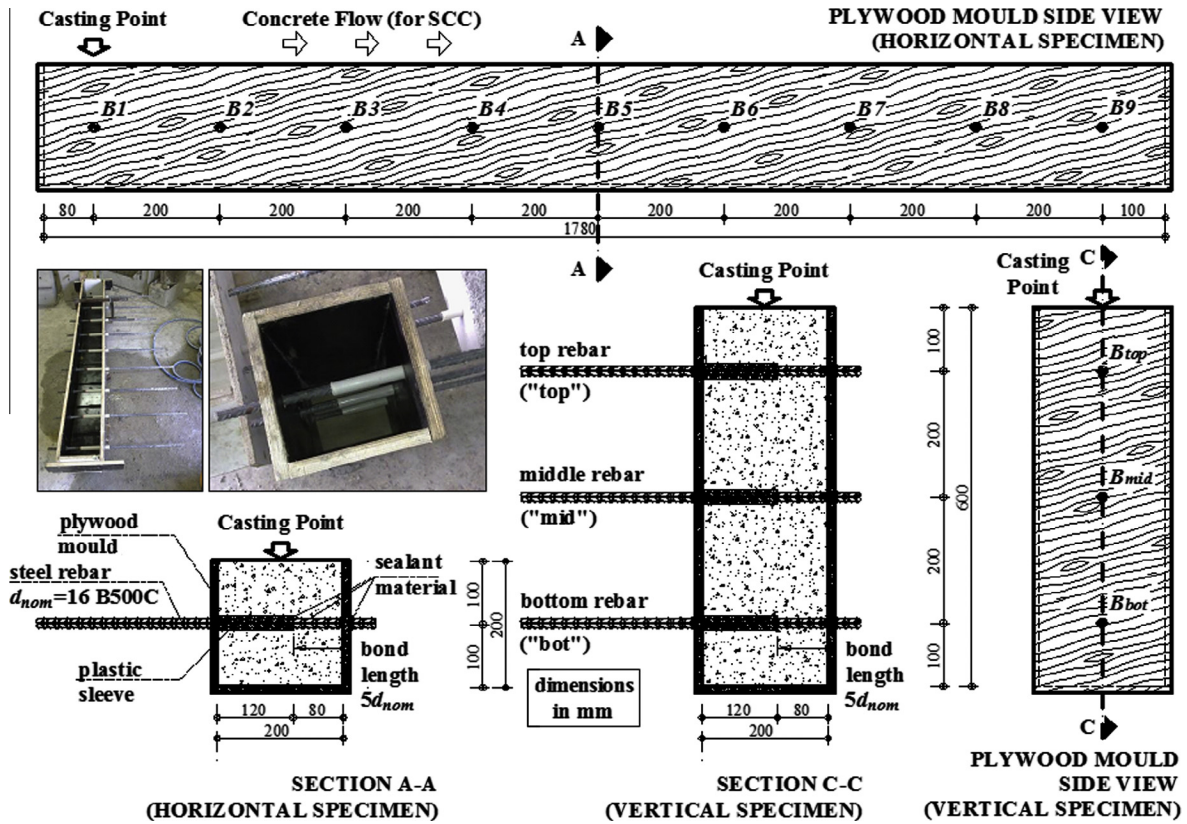


Fig. 4. Dimensions and setup of typical horizontal and vertical specimens.

Table 8
Summary of produced specimens and conducted tests.

| | SCC1 | SCC2 | SCC3 | SCC4 | SCC5 | SCC6 | SCC7 | NVC1 | NVC2 | NVC3 |
|---|------|------|------|------|------|------|------|------|------|------|
| Rheological characteristics | ● | ● | ● | ● | ● | ● | ● | ● | ● | ● |
| Compressive Strength | ● | ● | ● | ● | ● | ● | ● | ● | ● | ● |
| Bond | | | | | | | | | | |
| Vertical specimens | ● | ● | ● | ● | ● | ● | ● | ● | ● | ● |
| Horizontal specimens | ● | ● | × | × | ● | × | ● | ● | ● | ● |
| Rebar-to-concrete relative displacement during concrete setting | × | ● | × | × | ● | × | ● | × | ● | ● |

According to the applied standard, the plotted curve is a power function, in the form of Eq. (1), where PR is the penetration resistance (in N/mm^2), t the elapsed time from the beginning of hydration (in h) and 'a' and 'b' the regression analysis constants. It should be noted that higher values of 'a' or 'b' result in earlier times of initial setting.

$$PR = at^b \quad (1)$$

4.4. Effect of rebar displacements during concrete setting

In order to achieve a rebar-to-concrete relative displacement during setting, thus simulating the effect of a possible formwork displacement (Section 2.4), a bidirectional displacement of ± 5 mm was applied (Fig. 5) to specific rebars in part of the horizontal specimens (Table 8) at different moments, as specified in Table 9. It should be noted that the bidirectional displacement was applied in a continuous flow, without any dormant period between the consecutive stages. Specifically, an imposed rebar displacement was applied to each of the odd numbered bars B2, B4, B6 and B8 of the horizontal specimens, which were produced for mixtures SCC2, SCC5, SCC7, NVC2 and NVC3. The two first rebars, i.e. B2 and B4, were displaced before the initial setting time of concrete, whilst the two latter rebars, i.e. B6 and B8, were displaced in the period between the initial and the final setting times (Section 4.3).

4.5. Testing of specimens

At the end of the curing period (28 days), the cubic specimens were tested on a servo hydraulic compression frame, conforming to EN 12390-4 (2009) [49], in order to determine the cube compressive strength, f_{cc} (N/mm^2), according to EN 12390-3 (2009) [50].

The determination of the bond characteristics was performed in accordance with the Bond Test for Ribbed and Indented Reinforcing Steel (Pull-out Test) as described by Annex D of EN 10080 (2005) [36]. This test is based on RILEM Recommendation RC 6, as found in RILEM TC (1994) [51]. The pull-out test was conducted

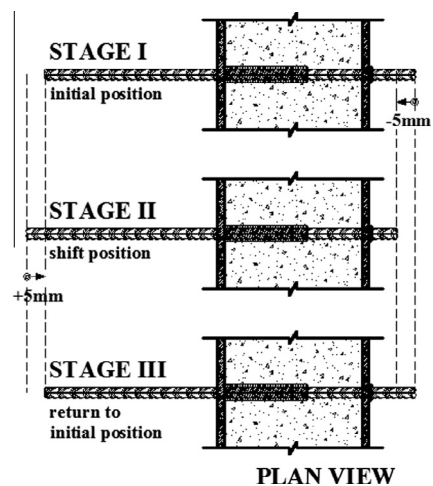


Fig. 5. Definition and application of rebar-to-concrete relative displacement.

Table 9
Time points of imposed displacements and setting times (in min from casting start).

| | SCC2 | SCC5 | SCC7 | NVC2 | NVC3 |
|-----------------|------|------|------|------|------|
| B2 | 230 | 295 | 477 | 65 | 90 |
| B4 | 350 | 320 | 632 | 80 | 145 |
| Initial setting | 395 | 347 | 635 | 97 | 147 |
| B6 | 395 | 355 | 652 | 105 | 165 |
| B8 | 410 | 365 | 662 | 130 | 180 |
| Final setting | 474 | 422 | 790 | 163 | 204 |

by applying a tensile force on the embedded reinforcement bar. The tension was applied to end of the steel rebar with the highest protruding length, while the other end of the rebar remained unstressed. The anchored part of the rebar was always set closer to the unstressed protruding end of the rebar.

The equipment arrangement of the test is illustrated in Fig. 6. For the application of the tensile force a hydraulic jack connected to a hydraulic pump was used. The pull-out force was progressively applied up to bond failure, while the corresponding slip of the rebar, s (mm), was recorded using three linear variable differential transformers (LVDTs) connected by a clamp to the unstressed protruding end of the rebar. A rigid steel plate was placed between the specimen and the hydraulic jack to act as a bearing plate and to ensure that the force is being applied uniformly to the face of the concrete surface. The applied axial force was acquired by a load cell of 300 kN capacity. All hardware parts were connected to a data acquisition system, which was recording the pull-out force versus the corresponding slips (relative displacement between steel and concrete) of the three LVDTs in real-time, at an acquisition rate of five measurements per second.

4.6. Result analysis procedures

4.6.1. Representative bond stresses

The bond stress, τ (N/mm²), at every different moment can be calculated using Eq. (2), where F (N) the applied force, $d_{nom} = 16$ mm the steel rebar diameter and $L = 80$ mm the nominal bond length of the rebar (Section 4.2), and be plotted as a function of the corresponding average slip s (mm) of the three LVDTs.

$$\tau = F/\pi d_{nom} L \quad (2)$$

A typical plot for all bars of one mixture, for both the vertical specimen (rebars B_{bot} , B_{mid} and B_{top}) and the horizontal specimen (rebars $B1$ to $B9$), is presented in Figs. 7 and 8, respectively. Four bond stresses were retained from each different curve (Fig. 9): $\tau_{0.01}$, $\tau_{0.10}$ and $\tau_{1.00}$, in respect to slip values $s = 0.01$, 0.10 and 1.00 mm, as well as the maximum bond stress, τ_{max} , at the time of the bond failure.

According to literature, the maximum (or ultimate) bond stress, τ_{max} , at the time of the bond failure and the ‘average’ bond stress, τ_m , were selected as representative stresses for the comparison of the mixtures. A significant number of studies [7–12,15–16,27,28] propose the use of τ_{max} due to its clear and univocal definition. The other representative value, τ_m , which is also widely used in literature [9,11,12,14] and is recommended by RILEM Recommendation RC 6 (append to RILEM TC 1994) [51], is calculated by using Eq. (3) as the arithmetic mean of bond stresses $\tau_{0.01}$, $\tau_{0.10}$ and $\tau_{1.00}$, corresponding to slips $s = 0.01$, 0.10 and 1.00 mm, respectively.

$$\tau_m = \frac{\tau_{0.01} + \tau_{0.10} + \tau_{1.00}}{3} \quad (3)$$

The bond capacity according to each of the above two representative bond stresses, normalized to the square root of the corresponding cube compressive strength of each mixture, $\tau/f_{cc}^{0.5}$ (τ and f_{cc} in N/mm²), in order to eliminate its effect on bond, is presented and compared in the results (Section 5.3).

4.6.2. Vertical specimens

For the vertical specimens and for each of the two representative bond stresses, a linear regression analysis (Fig. 10) was performed between the experimental bond stresses $\tau_{bot,exp}$, $\tau_{mid,exp}$ and $\tau_{top,exp}$ of the three tested rebars (dependent variable), i.e. B_{bot} , B_{mid} and B_{top} (Fig. 3), respectively, and their distance, H (m), from the bottom of the vertical specimen (independent variable). For the evaluation of the results the estimated values $\tau_{bot,est}$, $\tau_{mid,est}$ and $\tau_{top,est}$ are being henceforth used, as they are thought to be correcting any possible errors of the experimental values ($\tau_{bot,exp}$, $\tau_{mid,exp}$ and $\tau_{top,exp}$). For the simplification of the corresponding symbols, τ_{bot} , τ_{mid} and τ_{top} will be henceforth used instead of $\tau_{bot,est}$, $\tau_{mid,est}$ and $\tau_{top,est}$, respectively. For both representative stresses, τ_m and τ_{max} , the mixtures are being compared by the top-to-bottom rebar ratio, τ_{top}/τ_{bot} .

The acquired ratios were also evaluated on the basis of the adequacy of the major international building codes [1,2]. A 70% reduction of the bond strength of the bottom rebars is prescribed for rebars located in the upper ‘poor’ bond condition zone, above 250 of a 600 mm or deeper member, by EN 1992-1-1 [1]. Alternatively, a reinforcement location factor of 1.3 is applied by ACI 318 [2] for the calculation of the required rebar development length of rebars located above 300 mm of deep members. This location factor of the American Code leads to a reduction of the bond strength equivalent to the specifications of the European Code.

4.6.3. Horizontal specimens

For the horizontal specimens and for each of the two representative bond stresses, a linear regression analysis was performed between the bond stresses of the even numbered rebars (dependent variable), i.e. $B1$, $B3$, $B5$, $B7$ and $B9$ (Fig. 3), and their position across the length (independent variable). The estimated values are thought to be correcting any possible errors of the experiment, while the slope of the regression line presents the variation trend. It should be noted that for NVC mixtures, the regression line is ideally expected to be parallel to the length axis, as the concrete was cast at various points and the compaction was carefully applied and distributed over the whole specimen length. However, some variations are actually expected due the intrinsic variations of both the material and the testing procedures.

Using the resulting estimated values for both representative stresses, τ_m and τ_{max} , the mixtures are being compared by: (a) the slope of the linear regression curve and (b) the averages of the normalized bond stresses of the N tested bars of each horizontal specimen, $\tau_{avg}f_{cc}^{0.5}$, which were calculated according to Eq. (4). The odd numbered rebars $B2$, $B4$, $B6$ and $B8$ that were intentionally displaced during concrete setting (Section 4.4) were ignored during this analysis, but they were further compared to the measured values of the even numbers rebars $B1$, $B3$, $B5$, $B7$ and $B9$, in order to evaluate the effect of the imposed displacement of each odd rebar (at a given moment during concrete setting) on bond.

$$\tau_{avg}f_{cc}^{0.5} = \text{avg}(\tau/f_{cc}^{0.5})_N \quad (4)$$

One rebar was ignored, i.e. rebar $B5$ of NVC1, the surrounding concrete of which was damaged during the demoulding process.

4.6.4. Comparative analysis

In the last part of the analysis and for both representative stresses, τ_m and τ_{max} , the impact of the underlying and overlying material is being investigated by comparing $\tau_{avg}f_{cc}^{0.5}$ (Section 4.6.3) with the estimated bond stresses at the top

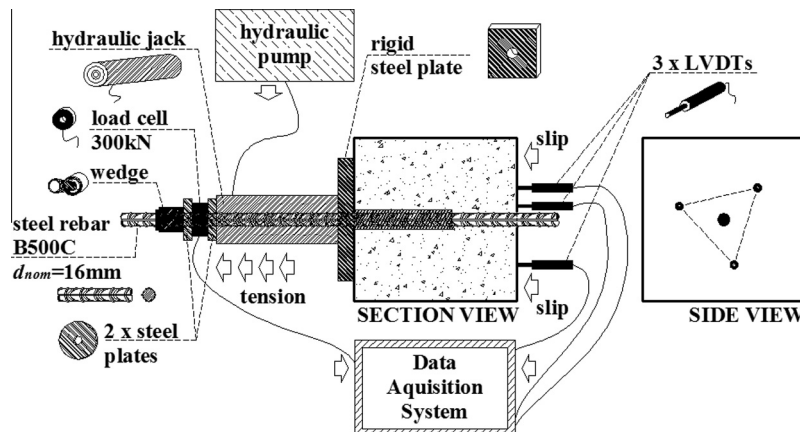


Fig. 6. Equipment description and arrangement for pull-out tests.

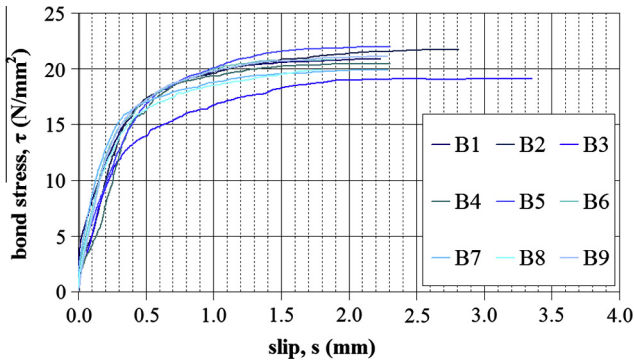


Fig. 7. Typical plot of bond stress as a function of slip for the horizontal specimen.

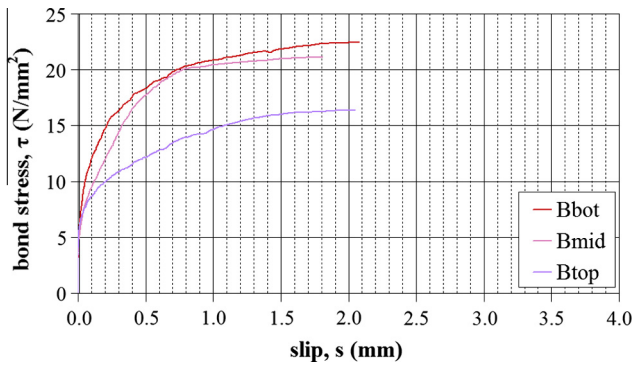


Fig. 8. Typical plot of bond stress as a function of slip for the vertical specimen.

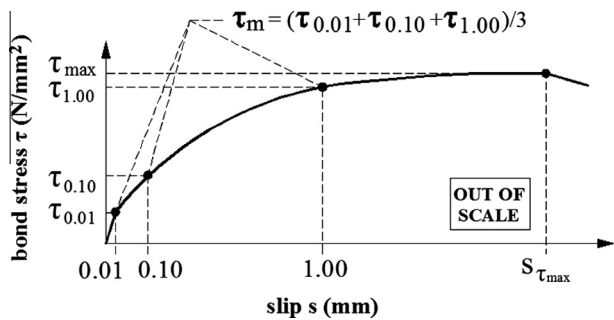


Fig. 9. Definition of the retained values.

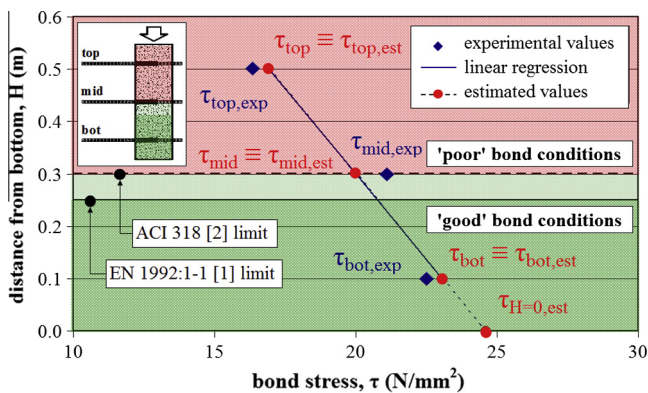


Fig. 10. Analysis procedure for vertical specimens (columns).

and bottom rebar of the vertical specimen, τ_{top} and τ_{bot} , respectively. The rebars of the horizontal specimens and the top rebars of the vertical specimens have the same overlying concrete layer thickness (100 mm), but different underlying layer thicknesses (100 and 500 mm, respectively). On the other hand, the rebars of the horizontal specimens and the bottom rebars of the vertical specimen have the same underlying layer thickness (100 mm), but different overlying layer thicknesses (100 and 500 mm, respectively). Therefore, the ratios τ_{top}/τ_{avg} and τ_{bot}/τ_{avg} are being evaluated, in order to investigate the effect of the underlying and overlying concrete layers on bond stress, respectively.

5. Results and discussion

5.1. Fresh properties & classification of mixtures

The results of the fresh concrete tests of all fresh SCC mixtures and the corresponding classification are shown in Table 10. It is reminded that, as described in Section 4.1, the *pce* content has been suitably adjusted, in order to reach the targeted fresh behaviour of the mixtures (flowability, viscosity and stability), as described in Section 4.1.

The examined SCC mixtures developed an average slump-flow diameter of 665 mm. It is recognised that higher deviations from the average value for some mixtures (e.g. SCC2 or SCC4) could have been further reduced by fine adjustment of the *pce* content. However, these deviations are not considered to have a significant impact in the examined mechanical characteristics of this study, given the fact that the other fresh properties strictly remain within the limits or the targeted rheological classes.

Specifically, the viscosity classes, as estimated by either the slump-flow times, t_{500} (s), or the V-funnel flow times, t_v (s), are common for this group of mixtures and all values are below the class change limits (2.0 s limit between VS1 and VS2 classes for Slump-flow time test, t_{500} , and 8.0 s limit between VF1 and VF2 classes for V-funnel test).

Furthermore, a satisfactory passing ability for all SCC mixtures is ensured by the obtained L-box ratios, *PL*, which are always equal or higher than the lower limit of the classification (0.80 for material passing through three smooth reinforcement bars).

All Fresh Visual Stability Indices, *FVSI*, were set to 0, due to the absence of signs of obvious dynamic segregation or bleeding. Thus, all SCC mixtures are considered to be stable.

As far as the NVC mixtures are concerned, three different workability classes were achieved, as shown in Table 11, by incorporating different *pce* levels.

5.2. Cube compressive strength

The decrease of the cube compressive strength, f_{cc} (N/mm²), due to the cement content reduction, is expected to be counterbalanced by the incorporation of *sf*. However, this was not observed in the experimental results. Specifically, as shown in Fig. 11, f_{cc} of the reference mixture was initially reduced for low *sf* replacement levels, before increasing again for higher *sf* levels of cement replacement.

As reported by Neville (2002) [52], the contribution of *sf* levels below 5% of the total mass of cementitious materials to strength may be insignificant, due to the fact the volume of *sf* is inadequate to cover the surface of all coarse aggregate particles and thus sufficiently enhance the interface zone between the aggregates and the paste, in terms of strength. In addition, it is considered that such *sf/b* replacement levels are considerably low to ensure the homogenous dispersion of the particles within the paste. As it is also reported in ACI 234R-06 [18], low *sf/b* replacement levels may reduce the water demand, as the *sf* particles will occupy space otherwise occupied by water between the cement particles. Therefore, the constant water content of the present study may be slightly higher than it would be actually required, thus further reducing the expected strength. However, it should be noted that

Table 10
Fresh properties and classification of SCC mixtures.

| Description | Symbol | SCC1 | SCC2 | SCC3 | SCC4 | SCC5 | SCC6 | SCC7 |
|------------------------------|----------------|------|------|------|------|------|------|------|
| Slump-flow | SF (mm) | 634 | 589 | 718 | 720 | 623 | 685 | 684 |
| Slump-flow class | | SF1 | SF1 | SF2 | SF2 | SF1 | SF2 | SF2 |
| Slump-flow time | t_{500} (s) | 0.8 | 1.6 | 0.6 | 0.9 | 1.4 | 0.5 | 1.6 |
| Viscosity class | | VS1 |
| V-funnel flow time | t_v (s) | 1.5 | 5.3 | 1.8 | 1.8 | 5.0 | 1.2 | 5.3 |
| V-funnel flow time 5 min | t_v 5min (s) | 1.5 | 7.9 | 2.0 | 1.9 | 5.8 | 2.0 | 6.6 |
| V-funnel viscosity class | | VF1 |
| L-box ratio | PL | 0.89 | 0.80 | 0.95 | 1.00 | 0.80 | 1.00 | 0.94 |
| Passing ability class | | PA2 |
| Fresh Visual Stability Index | FVSI | 0 | 0 | 0 | 0 | 0 | 0 | 0 |

Table 11
Fresh properties and classification of NVC mixtures.

| Description | Symbol | NVC1 | NVC2 | NVC3 |
|-------------|--------|------|------|------|
| Slump | S | 30 | 50 | 200 |
| Slump class | | S1 | S2 | S4 |

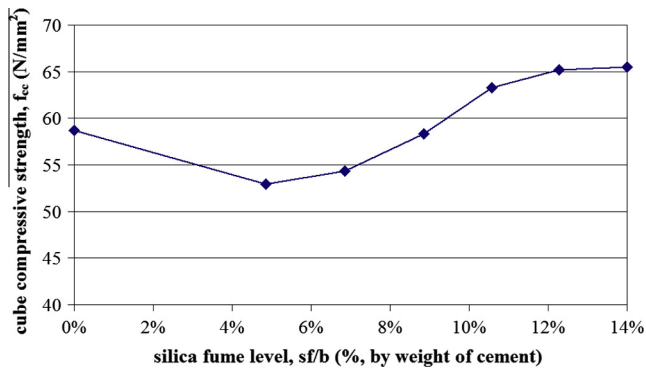


Fig. 11. Cube compressive strength as a function of the *sf/b* level (% by weight of cement).

this water demand reduction is not clearly quantified by any previous research study.

Summarising the above, it can be assumed that for low *sf/b* replacement levels, the incorporated *sf* is insufficient to contribute to strength and the cement reduction prevails in f_{cc} reduction (Fig. 11, decreasing branch up to approximately 5%), whereas for higher *sf/b* replacement levels, this f_{cc} reduction is counterbalanced by the incorporated *sf* (increasing branch between 5% and 14%). This rationale is qualitatively explained in Fig. 12. Specifically, the effect of the cement replacement by silica fume on the cube compressive strength (curve $f_{cc,A} + f_{cc,B}$) is provoked by the combined effect of (a) the gradual decrease (reduction) of the cement content, which is considered to result in a gradual smooth decrease of the compressive strength in the whole examined range (curve $f_{cc,A}$) and (b) the gradual increase (addition) of the silica fume (curve $f_{cc,B}$), which mainly enhances the compressive strength for levels above 5% (and up to the examined maximum level of 14%).

5.3. Bond properties

5.3.1. Effect of rebar position over height (top-bar effect)

As described previously (Section 4.6.2), the vertical specimens are being evaluated in terms of the occurrence and the significance of the top-bar effect.

In Fig. 13, the top-to-bottom bond stress ratios, τ_{top}/τ_{bot} , of all mixtures are comparatively presented for each of the two representative stresses, τ_m and τ_{max} . Ratios close to 1.0 designate a less

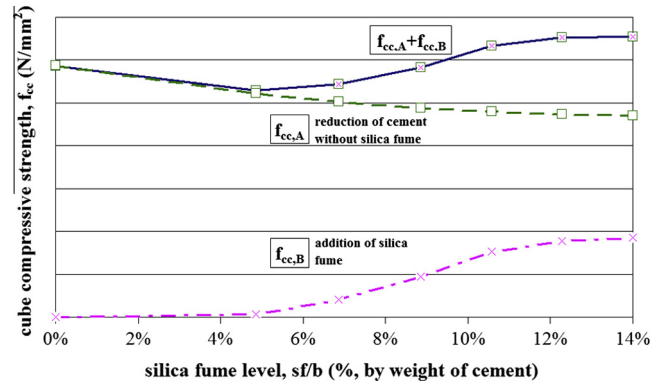


Fig. 12. Qualitative contribution of cement and silica fume to the cube compressive strength, for constant binder level.

significant top-bar effect, whereas ratios lower than 0.7 designate a more intense top-bar effect than the maximum prescribed by the building codes. As it can be observed, all SCC mixtures develop at least equal or higher ratios than NVC mixtures and they are always higher than the bond reduction ratio of 0.7 for poor bond conditions (Fig. 10), as assumed by EN 1992-1-1 (2004) [1]. This fact may be attributed to lower water and air accumulation beneath the reinforcement bars due to a possible densification of concrete-steel transition zone achieved by the incorporation of a higher fines (*lp*, *sf*) content and due to the lack of vibration, respectively.

The reference mixture SCC1 (*sf/b* = 0.0%) presents an insignificant loss of bond over height. A significant drop of the calculated ratio is evident for the lowest *sf/b* levels 4.9% and 6.9% (SCC2 and SCC3, respectively). The ratio is, then, gradually increased up to almost 1.0 for *sf/b* replacement levels between 8.9% and 10.6% (SCC4 and SCC5, respectively), which appear to express an

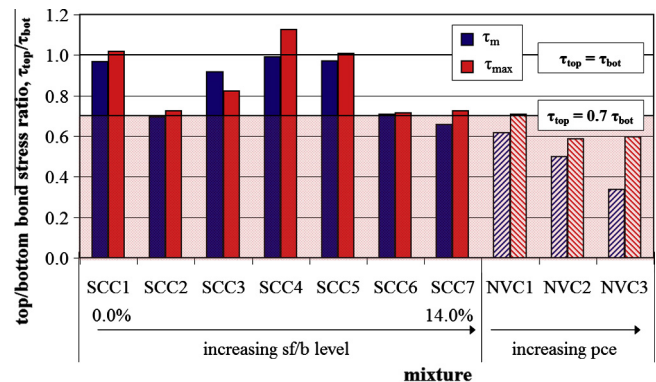


Fig. 13. Top-to-bottom bond stress ratio.

optimum level for the elimination of the top-bar effect in mixtures incorporating *sf* as a replacement material. For higher *sf/b* replacement levels (up to 14.0%) the ratio is again decreased, yet it is still higher than any of the NVC mixtures and at least equal to the code limit of 0.7. No significant differences are observed between ratios of SCC mixtures, calculated using τ_m or τ_{max} .

As far as NVC mixtures are concerned, a significant drop of the ratio, calculated for τ_m , is observed for higher levels of *pce* content. Specifically, higher *pce* levels appear to be significantly reducing τ_{top}/τ_{bot} ratio (from 0.60 to 0.35) for τ_m , whereas there seems to be a smoother and almost insignificant reduction for τ_{max} . It should be also highlighted that the bond reduction ratio of 0.7 appears to overestimate the experimental results, especially for τ_m and higher *pce* contents. However, it should be noted that the bond reduction ratio, as assumed by EN 1992-1-1 [1] refers to the design stresses and not the experimental values. Hence, the reduction ratio could be potentially adequate for NVC, but overestimated for SCC, so that a possible increase (e.g. to 0.8) for the latter concrete type may be reasonable. Further research is required to investigate the extent of this potential increase.

5.3.2. Effect of distance from the casting point

The effect of the rebar distance from the casting point on bond was examined by comparing the normalized bond stresses, $\tau_m/f_{cc}^{0.5}$ and $\tau_{max}/f_{cc}^{0.5}$, between the successive reinforcement bars across the length of the horizontal specimens (Fig. 3). The rebars that were intentionally displaced during concrete setting (Section 4.4) are ignored in this analysis.

In Figs. 14 and 15, no evident bond loss tendency is observed for either representative bond stress. The variations of both normalized representative stresses between the different rebars of each

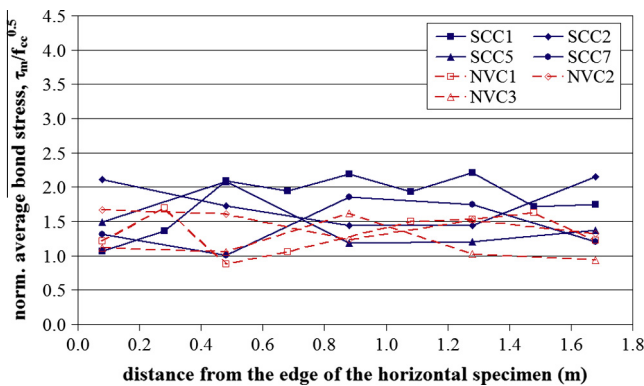


Fig. 14. Normalized average bond stress as a function of rebar position.

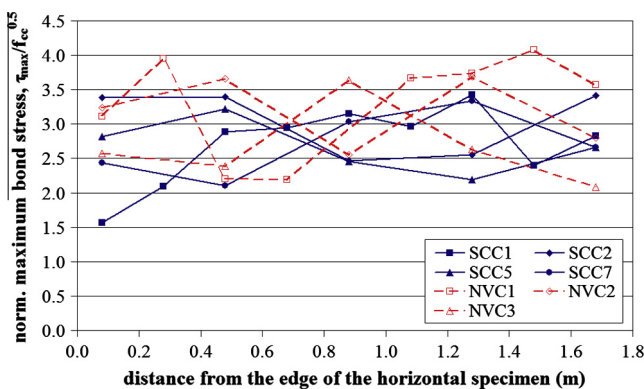


Fig. 15. Normalized maximum bond stress as a function of rebar position.

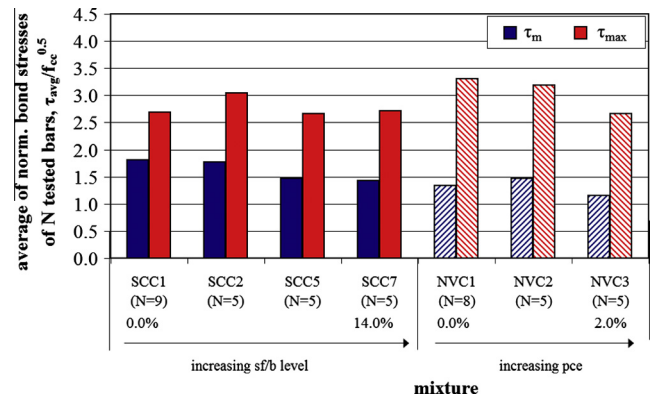


Fig. 16. Average of normalized representative bond stresses of *N* tested rebars.

SCC mixture appear to be comparable to the corresponding variations of the NVC mixtures. These variations are attributed to the intrinsic variations of both the material and the testing procedures. Thus, it can be concluded that the absence of mechanical compaction and the free flow of fresh SCC do not seem to affect the resulting bond stress for the measured distance from the casting point (1.60 m between rebars B1 and B9, Fig. 3).

This finding may imply that for bidirectional or multidirectional casting in linear or surface members, respectively, a single casting point may only be required for a total length of at least 3.20 m (casting point in the middle of a linear member: 2 × 1.60 m) or a total surface of at least 10.24 m² (casting point in the centre of a square region: 3.20 m × 3.20 m). However, although not experimentally investigated, it is considered that higher member congestion, higher member lengths or mixtures with different viscosity may significantly influence the results and the effects of such alterations have to be further examined.

Based on the previous findings, the comparative investigation of the averages of the normalized bond stresses of *N* tested non-displaced rebars of each mixture, as described in Section 4.6.3, can be considered as safe to conduct.

This comparison is shown in Fig. 16. It can be observed that for τ_m the average normalized bond stress is at least equal or higher than the corresponding values of NVC, regardless of the *sf* level. On the other hand, for τ_{max} , the average normalized bond stress appears to be higher for NVC. This observation of the contradictory results, depending on the selection of the representative stress (τ_m or τ_{max}), has been further discussed elsewhere [23,30,53]. Specifically, it has been found the representative stress selected for the comparison between SCC and NVC may play an important role on the extracted conclusions. In particular, the average stress (τ_m) appears to be higher in SCC, whereas the maximum stress (τ_{max}) appears to be higher in NVC.

5.3.3. Effect of the underlying and overlying concrete layers

The impact of the underlying and overlying concrete layers on bond stress is presented in Figs. 17 and 18, respectively. Specifically, the bond stresses of the top and the bottom rebar of the vertical specimens are compared to the corresponding average stress of the horizontal specimens (of the same mixture) by evaluating the ratios τ_{top}/τ_{avg} and τ_{bot}/τ_{avg} , respectively. Ratios closer to 1.0 imply an insignificant effect of the underlying or overlying concrete layer. It was observed that the effects of either τ_m or τ_{max} are similar, thus they will not be separately discussed.

It is evident that for SCC1 both the underlying and the overlying layer do not affect the bond stress. The lowest *sf* level (4.9% for SCC2) appears to decrease τ_{top}/τ_{avg} (Fig. 17), by approximately 40%. The ratio is again increased almost to 1.0 for a replacement

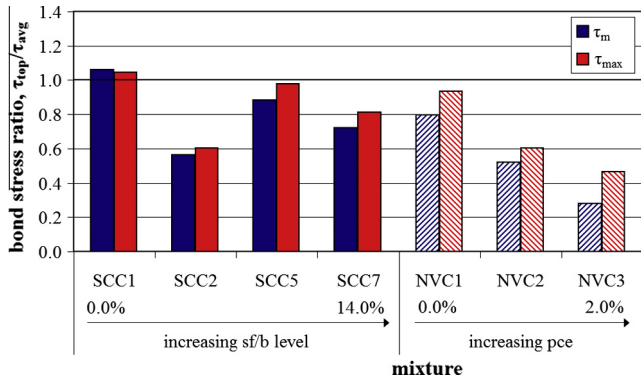


Fig. 17. Impact of the underlying concrete layer on bond stress.

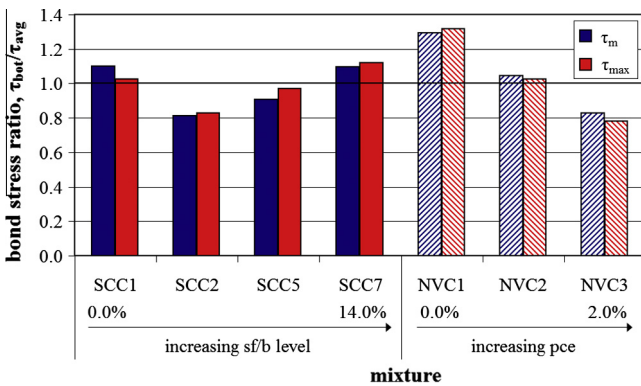


Fig. 18. Impact of the overlying concrete layer on bond stress.

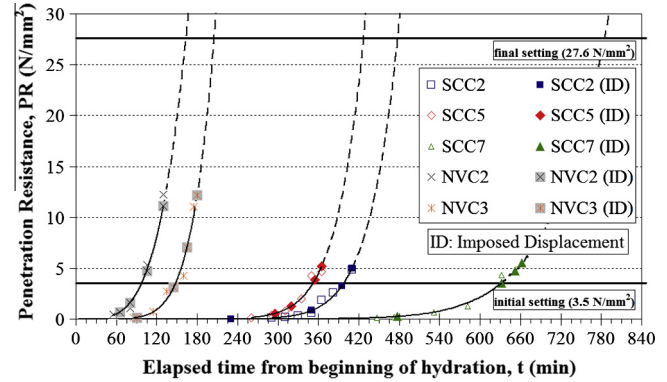


Fig. 19. Penetration resistance as a function of the elapsed time from the beginning of hydration.

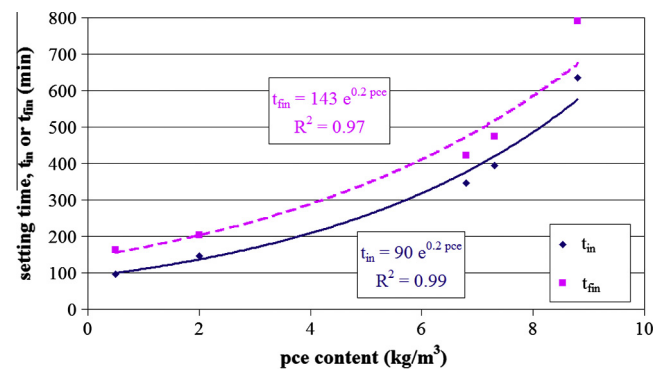


Fig. 20. Concrete setting times as a function of the pce content.

level of 10.6% (SCC5), before being again decreased for further cement replacement. For NVC mixtures, the underlying concrete layer appears to play an important role for higher pce content. Specifically, τ_{top}/τ_{avg} is significantly decreased for higher pce content, regardless of the representative stress.

The overlying layer seems to offer a better compaction to the bottom rebar for mixtures SCC1 (absence of sf) and SCC7 (high sf content), as illustrated by τ_{bot}/τ_{avg} ratios greater than 1.0 (Fig. 18). The enhancing effect is reduced for the lowest sf level (4.9% for SCC2), but is gradually increased for higher sf/b levels. For NVC, the positive effect of the overlying layer is more pronounced for lower pce content of NVC mixtures.

5.3.4. Concrete setting

The increase of the penetration resistance during concrete setting is found to be excellently reflected ($R^2 > 0.97$) by the power regression (Eq. (1)) for all tested mixtures. The power curves are presented in Fig. 19. It is evident that SCC mixtures develop higher initial setting times, varying from approximately 4 to 9 h later than the corresponding times for NVC mixtures.

This delay is ascribed to the high pce content of SCC mixtures, required to achieve the desired fresh concrete properties. Specifically, both setting times, t_{in} and t_{fin} (min), are very well correlated to the pce content, as shown in Fig. 20.

5.3.5. Effect of rebar displacements during concrete setting

In Figs. 21 and 22, the average and the maximum bond stresses of each intentionally displaced rebar B_i ($i = 2, 4, 6$ or 8, Section 4.4), τ_{B_i} , during concrete setting are compared to the corresponding average values, τ_{avg} , of the non-displaced bars (B1, B3, B5, B7 and B9) of the horizontal specimens, as they were calculated in Sec-

tion 5.3.2. By calculating the τ_{B_i}/τ_{avg} ratio (for τ_m or τ_{max}), the effect of the relative displacement between rebars and the surrounding concrete, due to unintentional formwork displacements, on bond can be evaluated. Ratios greater than 1.0 illustrate a positive effect, in the sense that a better compaction is achieved in the region of the concrete-steel interface. The composition variations do not seem to be reflected in the results for either type of concrete, SCC or NVC.

It is evident (Fig. 21) that a rebar-to-concrete relative displacement at different moments before the initial setting (reinforcement bars B2 and B4), have different effects on τ_m of the two concrete types. For both NVC mixtures, a significantly better compaction is achieved for rebar B2 (very early imposed rebar displacement), leading to a 40% higher bond stress. Then, the bond stress is gradually decreased down to 20–30% of its initial value. On the other hand, no significant effect is observed for either rebar of SCC mixtures before the initial setting. The bond stress of rebar B6 is then reduced to about 40–50% of τ_{avg} for all mixtures. A slight enhancement of the bond stress is observed for the corresponding stress of rebar B8, a fact that is mainly evident for SCC7. Considering that for this mixture, the moments of the displacement application on rebars B6 and B8 were very close to each other (Fig. 19), it is assumed that this difference is due to intrinsic variation of the material and the testing procedures. The bond loss after the initial setting is considered to be practically constant for B6 and B8 and lower for SCC mixtures (between 30% and 60% for SCC compared to 60–80% for NVC).

Similar findings are evident for τ_{max} of all SCC mixtures and the first two rebars, B2 and B4 (Fig. 22). The reduction of the representative stress τ_{max} is again practically similar for rebars B6 and B8 (from 20% to 50%). For NVC mixtures, the earliest displacement (B2) offers a better compaction, yet less significant compared to

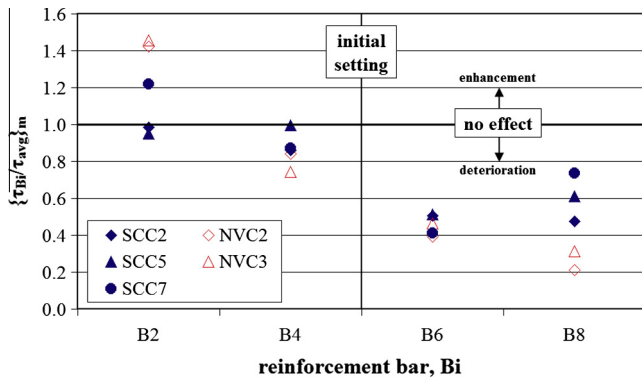


Fig. 21. Impact of rebar-to-concrete relative displacement on τ_m at different times during concrete setting.

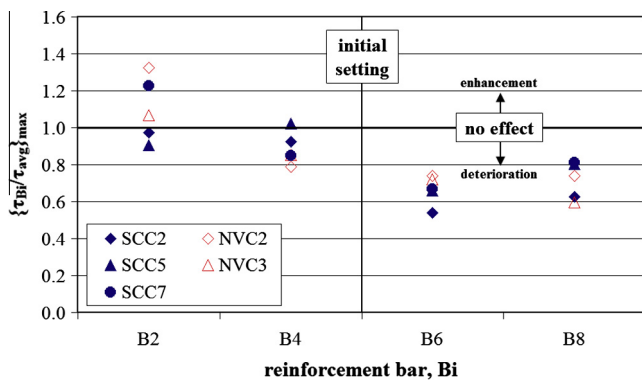


Fig. 22. Impact of rebar-to-concrete relative displacement on τ_{max} at different times during concrete setting.

the corresponding effect for τ_m . The stress is then gradually decreased down to 60–80% of its initial value for rebars B6 and B8, which appear to have an almost common behaviour. This decrease is significantly smoother than for the case of τ_m .

Summing up the above findings, SCC appears to have a better overall behaviour than NVC until the initial setting time. Although the high *pce* content in SCC mixtures results in a considerable delay of the initial setting, any seismic events occurring during this larger period after casting are not expected to have any negative effect on bond capacity. After the initial setting, the two concrete types present a resembling reduction of the bond stress, which for τ_m is slightly lower in SCC than in NVC mixtures.

6. Conclusions

The investigation of the effect of silica fume content, as a replacement material of cement, on special bond parameters of typical stable SCC mixtures with a common composition and similar flowability and viscosity was the incentive of the present study. Similar variations of silica fume content for different common compositions of SCC are expected to result in similar trends of bond parameters. A comparison with typical NVC mixtures was also performed. It has been found that:

- Low *sf/b* levels in SCC appear to be inadequate to contribute to f_{cc} . The contributing action is pronounced for *sf/b* levels higher than 6.9%.
- The top-bar effect is always less intense for SCC incorporating silica fume, compared to NVC and it is almost eliminated for SCC mixtures with *sf/b* levels between 8.9% and 10.6%. An

increase of the bond reduction ratio, as assumed by codes, can be potentially considered, based on future targeted research.

- The effect of the underlying concrete layer is less significant (a) for SCC incorporating silica fume (compared to NVC) (b) for SCC mixtures with *sf/b* levels around 10% and (c) for NVC mixtures with lower *pce* content. On the other hand, the effect of the overlying concrete layer is less significant (a) for SCC incorporating silica fume (compared to NVC), (b) for SCC mixtures with higher *sf/b* levels and (c) for NVC mixtures with lower *pce* content.
- For SCC mixtures, no bond loss is evident for distances from the casting point up to at least 1.60 m (measured distance in the present study), whilst a comparable bond variation to NVC mixtures is calculated. Thus, linear SCC members up to 3.20 m or surface members of approximately 10 m², cast with a single centric casting point are expected to present constant bond behaviour. However, high congestion or higher distances from the casting point may influence this ability and have to be investigated further.
- Concrete setting depends on the *pce* content, regardless of the concrete type. A rebar-to-concrete relative displacement due to unintentional formwork displacements occurring during the longer period up to the initial setting of SCC (compared to NVC) is not expected to negatively influence bond capacity. After the initial setting of concrete, the negative effect of a relative displacement between rebars and concrete due to unintentional formwork displacements on bond is almost similar between SCC and NVC.

Acknowledgements

Authors would like to thank (in alphabetical order) BASF Hellas, Dionysosmarble Group, Halysourgiki Inc. and Interbeton Building Materials S.A. for providing the raw materials for the production of the concrete mixtures. Gratitude should also be expressed to Prof. S. Koliass and Lect. E. Badogiannis for their flourishing scientific advice.

References

- [1] EN 1992-1-1. Design of concrete structures. Part-1-1: General rules and rules for buildings. European Committee for Standardization; 2004.
- [2] ACI 318/318R. Building code requirements for structural concrete (318) and commentary (318R). Farmington Hills (MI, USA): American Concrete Institute; 2008.
- [3] Ozawa K, Maekawa K, Kunishima M, Okamura H. Development of high performance concrete based on the durability design of concrete structures. In: Proceedings of the 2nd East-Asia & Pacific conference on structural engineering and construction (EASEC-2), vol. 1; 1989. p. 445–50.
- [4] Okamura H, Maekawa K, Ozawa K. High performance concrete. Gihodo Publishing; 1993.
- [5] Maekawa K, Ozawa K. Development of SCC's prototype. Self-compacting high-performance concrete. Social System Institute; 1999. p. 20–32 [in Japanese].
- [6] Okamura H, Ouchi M. Self-compacting concrete (Invited Paper). J Adv Concr Tech 2003;1(1):5–15.
- [7] Zhu W, Sonebi M, Bartos PJM. Bond and interfacial properties of reinforcement in self-compacting concrete. Mater Struct 2004;37:442–8.
- [8] Castel A, Vidal T, Viriyametanont K, Francois R. Effect of reinforcing bar orientation and location on bond with self-consolidating concrete. ACI Struct J 2006;103(4):559–67.
- [9] Almeida Filho FM, El Debs MK, El Debs ALHC. Bond-slip behavior of self-compacting concrete and vibrated concrete using pull-out and beam tests. Mater Struct 2008;41:1073–89.
- [10] Hassan AAA, Hossain KMA, Lachemi M. Bond strength of deformed bars in large reinforced concrete members cast with industrial self-consolidating concrete mixture. Constr Build Mater 2009;24:520–30.
- [11] Valcuende M, Parra C. Bond behaviour of reinforcement in self-compacting concretes. Constr Build Mater 2009;23:162–70.
- [12] Desnerck P, De Schutter G, Taerwe L. Bond behaviour of reinforcing bars in self-compacting concrete: experimental determination by using beam tests. Mater Struct 2010;43:53–62.

- [13] Thrane LN, Pade C, Idzerda C, Kaasgaard M. Effect of rheology of SCC on bond strength of ribbed reinforcement bars. In: Khayat KH, Feys D, editors. Proceedings of SCC2010 RILEM conference, Montreal, Canada, September 26–29, RILEM book series 1. New York: Springer; 2010. p. 367–78. http://dx.doi.org/10.1007/978-90-481-9664-7_30.
- [14] Trezos KG, Sfikas IP, Pasios CG. Influence of water-to-binder ratio on top-bar effect and bond variation across length in self-compacting concrete specimens. *Cem Concr Compos* 2014;48:127–39. <http://dx.doi.org/10.1016/j.cemconcomp.2013.11.012>.
- [15] Khayat KH, Manai K, Trudel A. In situ mechanical properties of wall elements cast using self-consolidating concrete. *ACI Mater J* 1997;94(6):491–500.
- [16] Chan YW, Chen YS, Liu YS. Development of bond strength of reinforcement steel in self-consolidating concrete. *ACI Struct J* 2003;100(4):490–8.
- [17] Cairns J, Plizzari GA. Towards a harmonized European bond test. *Mater Struct* 2003;36:498–506.
- [18] ACI 234R. Guide for the use of silica fume in concrete. American Concrete Institute; 2006.
- [19] Pop I, De Schutter G, Desnerck P, Onet T. Bond between powder type self-compacting concrete and steel reinforcement. *Constr Build Mat* 2013;41:824–33. <http://dx.doi.org/10.1016/j.conbuildmat.2012.12.029>.
- [20] Gjørsv OE, Monteiro PJM, Mehta PK. Effect of condensed silica fume on the steel–concrete bond. *ACI Mater J* 1990;87(6):573–80.
- [21] Domone PL. A review of the hardened mechanical properties of self-compacting concrete. *Cem Concr Compos* 2007;29:1–12.
- [22] Aslani F, Nejadi S. Bond behavior of reinforcement in conventional and self-compacting concrete. *Adv Struct Eng – Int J* 2012;15(12):2033–51.
- [23] Sfikas I, Trezos K. Effect of composition variations on bond properties of self-compacting concrete specimens. *Constr Build Mat* 2013;41:252–62.
- [24] Sellevold EJ, Nilsen T. Condensed silica fume in concrete: a world review. In: Malhotra VM, editor. *Supplementary cementing materials for concrete*. Ottawa, Canada: CANMET; 1987. p. 165–243.
- [25] Ezeldin A, Balaguru P. Bond behavior of normal and high-strength fiber reinforced concrete. *ACI Mater J* 1989;86(5):515–24.
- [26] Abadjiev P, Panayotov K, Petrov SI. Influence of condensed silica fume as admixture to concrete on the bond to the reinforcement. *Constr Build Mat* 1993;7(1):41–4.
- [27] Söylev TA, François R. Effects of bar–placement conditions on steel–concrete bond. *Mater Struct* 2006;39:211–20.
- [28] Esfahani MR, Lachemi M, Kianoush MR. Top-bar effect of steel bars in self-consolidating concrete. *Cem Concr Compos* 2008;30:52–60.
- [29] Hossain KMA, Lachemi M. Bond behavior of self-consolidating concrete with mineral and chemical admixtures. *ASCE J Mater C Eng* 2008;20(9):608–16.
- [30] Trezos K, Sfikas I, Pamos M, Sotiropoulou E. Top-Bar Effect in Self-Compacting Concrete Elements. In: design, production and placement of self-consolidating concrete. In: Khayat KH, Feys D, editors. Proceedings of SCC2010 RILEM conference, Montreal, Canada, September 26–29, RILEM book series 1. New York: Springer; 2010. p. 367–78. http://dx.doi.org/10.1007/978-90-481-9664-7_30.
- [31] ACI 237R. Self-consolidating concrete. American Concrete Institute; 2007.
- [32] EN 206. Concrete – Part 1: specification, performance, production and conformity. European Committee for Standardization; 2007.
- [33] EN 197-1. Cement – Part 1: composition, specifications and conformity criteria for common cements. European Committee for Standardization; 2011.
- [34] EN 1097-6. Tests for mechanical and physical properties of aggregates – Part 6: determination of particle density and water absorption. European Committee for Standardization; 2000.
- [35] EN 934-2. Admixtures for concrete, mortar and grout – Part 2: concrete admixtures. Definitions, requirements, conformity, marking and labelling. European Committee for Standardization; 2009.
- [36] EN 10080. Steel for the reinforcement of concrete. European Committee for Standardization; 2005.
- [37] Desnerck P, De Schutter G, Taerwe L. A local bond stress-slip model for reinforcing bars in self-compacting concrete. In: Oh BH et al., editors. *Fracture mechanics of concrete and concrete structures – assessment, durability, monitoring and retrofitting of concrete structures*. Seoul: Korea Concrete Institute; 2010. ISBN 978-89-5708-181-5.
- [38] Helincks P, Boel V, De Corte W, De Schutter G, Desnerck P. Structural behaviour of powder-type self-compacting concrete: bond performance and shear capacity. *Eng Struct* 2013;48:121–32. <http://dx.doi.org/10.1016/j.engstruct.2012.08.035>.
- [39] EN 12350-8. Testing fresh concrete – Part 8: self-compacting concrete – slump-flow test. European Committee for Standardization; 2010.
- [40] ASTM C1611. Standard test method for slump flow of self-consolidating concrete. Annual book of ASTM standards. Section 04, V04.02: Concrete and Aggregates; 2007.
- [41] EN 12350-9. Testing fresh concrete Part 9: self-compacting concrete – V-funnel test. European Committee for Standardization; 2010.
- [42] EN 12350-10. Testing fresh concrete Part 10: self-compacting concrete – L-box test. European Committee for Standardization; 2010.
- [43] EN 12350-2. Testing fresh concrete – Part 2: slump test. European Committee for Standardization; 2009.
- [44] ASTM C 138. Standard test method for density (unit weight), yield, and air content (gravimetric) of concrete; 2001.
- [45] BIBM, CEMBUREAU, EFCA, EFNARC, ERMCO. European guidelines for self-compacting concrete: specification, production and use; 2005.
- [46] EN 12390-2. Testing hardened concrete – Part 2: making and curing specimens for strength tests. European Committee for Standardization; 2009.
- [47] EN 13670. Execution of concrete structures. European Committee for Standardization.
- [48] ASTM C 403. Standard test method for time of setting of concrete mixtures by penetration resistance. PA: American Society for Testing and Materials; 1999.
- [49] EN 12390-4. Testing hardened concrete – Part 4: compressive strength. specification for testing machines. European Committee for Standardization; 2009.
- [50] EN 12390-3. Testing hardened concrete – Part 3: compressive strength of test specimens. European Committee for Standardization; 2009.
- [51] RILEM TC. RILEM recommendations for the testing and use of constructions materials, RC 6 bond test for reinforcement steel. 2. Pull-out test, 1983, E & FN SPON; 1994. p. 218–20.
- [52] Neville AM. *Properties of concrete: fourth and final edition (standards updated to 2004)*. Pearson Education Limited; 2004.
- [53] Sfikas I, Trezos K. Impact of water to binder ratio and silica fume content on bond properties of self-compacting concrete cube specimens. In: Proceedings of the 4th international symposium: bond, anchorage, detailing (BIC 2012), fib, RILEM, 17–20 June. Italy: University of Brescia; 2012.